THE JOURNAL OF PHYSICAL CHEMISTRY C

pubs.acs.org/JPCC

Article

# Structural Stability of Physisorbed Air-Oxidized Decanethiols on Au(111)

Özlem Kap,[¶] Nikolai Kabanov,[¶] Martina Tsvetanova, Canan Varlikli, Andrey L. Klavsyuk, Harold J. W. Zandvliet, and Kai Sotthewes*

Cite This: *J. Phys. Chem. C* 2020, 124, 11977−11984

Read Online

ACCESS | Metrics & More | Article Recommendations

**ABSTRACT:** We have studied the dynamic behavior of decanethiol and air-oxidized decanethiol self-assembled monolayers (SAMs) on Au(111) using time-resolved scanning tunneling microscopy at room temperature. The air-oxidized decanethiols arrange in a lamellae-like structure leaving the herringbone reconstruction of the Au(111) surface intact, indicating a rather weak interaction between the molecules and the surface. Successive STM images show that the air-oxidized molecules are structurally more stable as compared to the nonoxidized decanethiol molecules. This is further confirmed by performing current−time traces with the feedback loop disabled at different locations and at different molecular phases. Density function theory calculations reveal that the diffusion barrier of the physisorbed oxidized decanethiol molecule on Au(111) is about 100 meV higher than the diffusion barrier of a chemisorbed Au-decanethiol complex on Au(111). A two-dimensional activity map of individual current−time traces performed on the air-oxidized decanethiol phase reveals that all the dynamic events take place within the vacancy lines between the air-oxidized decanethiols. These results reveal that the oxidation of thiols provides a pathway to produce more robust and stable self-assembled monolayers at ambient conditions.

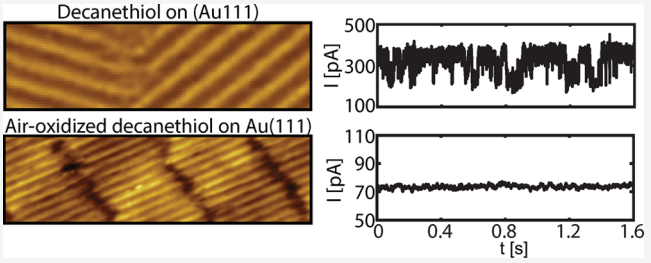


## INTRODUCTION

Surface modification of metal substrates via adsorption of organic molecules to form self-assembled monolayers (SAMs) has been extensively studied due to the easy fabrication of a uniform functional surface over a wide area.[1−3] In order to integrate SAMs into functional devices, such as biosensors or molecular electronics,[4−6] a fundamental and detailed understanding of the structural and electronic properties, dynamics, and molecular interactions is required. The most popular model systems for self-assembly are alkanethiols on Au(111) substrates because of their convenient preparation by chemisorption from dilute solutions. In addition, the alkanethiol SAMs provide well-defined structures with tunable interfacial properties.[7−10]

The mobility and stability of thiolates on surfaces has important implications for applications of SAMs, for instance, in the spreading of alkanethiol molecules in microcontact printing[11] or on the surface of thiolate-protected nanoparticles and clusters.[12] Therefore, fundamental research on SAMs on flat gold can provide valuable insights into the development of stable thiolate SAM coatings for two-dimensional device architectures and for the stabilization of nanoparticles and clusters. Several experiments have shown that alkanethiol SAMs undergo phase transitions and dynamic events at room temperature, indicating that the gold−thiolate interface of thiolate SAMs on Au(111) is not rigid.[13−18]

Oxidation of the gold−thiolate bond when exposed to air, UV light, or elevated temperatures leads to degradation of the thiolate monolayer.[18−23] After these findings, it was concluded that light and the presence of oxygen, with ozone being the main oxidant, could remove alkanethiolate SAMs from the gold surface.[22,24,25] The rate of oxidation depends on the morphology of the surface, the concentration of oxidants (e.g., ozone) in the ambient atmosphere, and the alkyl chain length.[26−29] When oxidized, the SAMs lose their ordered, oriented upright nature and form lying-down ($\lambda$ phase) or disordered phases.[15,18,25] In a recent study, Sotthewes et al.[18] demonstrated, using X-ray photoelectron spectroscopy (XPS), scanning tunneling microscopy (STM), and molecular dynamics (MD) simulations, that alkanesulfonates (i.e., oxidized alkanethiols) arrange in a lamellae-like structure without affecting the herringbone reconstruction of the

**Received:** March 30, 2020
**Revised:** May 5, 2020
**Published:** May 5, 2020

Au(111) surface, indicating that the interaction between the molecules and the surface is rather weak.

There have been numerous studies regarding the structure of alkanethiol SAMs on Au substrates. The structure of the SAMs depend on coverage, temperature, and crystal orientation of the substrate. In total, over ten different phases have been observed. The most common ones are the centered $(23\times\sqrt{3})$ phase ($\beta$), the hexagonal $(5\sqrt{3}\times\sqrt{3})$R30° phase ($\delta$) and the centered $(3\times2\sqrt{3})$ standing-up phase ($\phi$), which is found at full coverage. After oxidation, only low-density lying-down alkanethiol phases are observed on the surface in coexistence with the alkanesulfonate phase together with antiphase boundaries, vacancy islands, and ad-islands.[8−10,30,31] In these various phases, the molecules arrange in different adsorption configurations, affecting not only the interfacial properties but also the dynamic properties, such as diffusion, flipping of the tail,[16] planar rotation,[32,33] or bond breaking and remaking.[34] With the help of current−time spectroscopy ($I(t)$), it is possible to characterize the dynamic events.[16,33,35]

Here we investigate the structural stability of the decanethiol and air-oxidized decanethiol (decanesulfonates) SAMs by space- and time-resolved scanning tunneling microscopy. We reveal that the physisorbed decanesulfonate phase exhibits fewer dynamic events and is structurally more stable compared to the chemisorbed decanethiol phase. Within the decanethiol phase, phase transitions occur between the ordered $\beta$ phase and a disordered phase, while almost no dynamic events are observed in the decanesulfonate phase. In addition, a limited amount of molecular exchange is observed between the decanethiol and decanesulfonate phases. Density function theory (DFT) simulations reveal that the diffusion barrier of the physisorbed oxidized decanethiol molecule on Au(111) is about 100 meV higher than the diffusion barrier of a chemisorbed decanethiol molecule on Au(111), opposite to the calculated binding energies.[36,37] A two-dimensional activity map reveals that all the dynamics within the decanesulfonate phase are observed within the vacancy lines between the molecules. The switching process is stochastic and is caused by the small displacement of the sulfonate part of the molecule. For the decanethiol phase also, stochastic switching is observed; only the switching events are delocalized.

## METHODS

**Experimental Details.** Decanethiol (purity ≥ 99%) was purchased from Sigma-Aldrich (Germany) and used without further purification. Au(111) was purchased commercially from Phasis (Switzerland). The substrates were cleaned prior to immersion by a copious amount of ethanol (purity ≥ 99%, Sigma-Aldrich), 2-propanol from Merck (Germany), and purified water. The cleaned gold substrates were immersed with minimal delay into a a 1 mM ethanolic solution for 1 h. This immersion step leads to a densely packed SAM where the decanethiolate molecules form a standing-up phase. In order to reduce the coverage, we immersed our sample in a pure ethanol solution for 1 h. Oxidation of the monolayer was obtained by storing the sample in a wooden container (preventing exposure of light onto the sample but allowing air in) for 2 weeks under ambient laboratory conditions (20 °C and 37 ± 1% humidity, measured with a ENSIRION EK-H4 SHTXX, Humidity Sensors, Eval Kit, SENSIRION, Switzerland). For more details, see ref 18. Subsequently, the samples were loaded into a UHV STM for imaging (RHK Technology UHV3000 variable temperature STM operating at a base pressure of $1\times10^{-10}$ mbar, using chemical etched W tips). All measurements are acquired at room temperature.

**Analysis Details.** A home-built MATLAB program has been used to analyze the areal fractions. The step-edges are determined by the Canny edge detection method. Based on these step edge positions, the terraces are identified and subsequently we have analyzed all terraces separately. The disordered regions are identified by subtraction of the original image from a Gaussian filtered image. The $\beta$-phase regions are identified using the Canny edge detection method with a lower threshold value (based on the substantial difference in corrugation of the $\beta$ and $\lambda$ phase). The remaining areas are $\lambda$ phase regions. Regarding the island content analysis: the island is manually cropped out of the image. The island is surrounded by the $\lambda$ phase. The island only contains the $\beta$ phase and disordered regions, which are detected by the methods mentioned above.

**Computational Details.** *Ab initio* density functional calculations of activation barriers for diffusion of decanethiol and air-oxidized decanethiol were performed using the projector augmented-wave (PAW) technique,[38,39] as implemented in the Vienna ab initio simulation package (VASP).[40] We used the GGA-PBE density functional[41] and a plane-wave basis set with a kinetic energy cutoff of 400 eV. The substrate has been modeled as periodically repeated slabs consisting of up to three atomic layers separated by a sufficiently thick vacuum space. The bottom layer of the slab is fixed and the top two layers are allowed to relax upon optimization. A $(1\times4\times1)$ Monkhorst−Pack k-point grid[42] is used in all our calculations to sample the Brillouin zone of the surface unit cell. The contributions of van der Waals forces were estimated using dDsC dispersion corrections.[43] To study the diffusion of decanethiol and air-oxidized decanethiol on the Au(111) surface, we employed the nudged elastic band method[44,45] implemented in VASP to locate the saddle points of the potential energy surface and search for the minimum energy pathway of diffusion. The minimum energy path was discretized by nine intermediate states between fcc and hcp states. The atomic models are drawn using VESTA.[46]

## RESULTS AND DISCUSSION

In Figure 1A−D, a sequence of STM images of an air-oxidized decanethiol self-assembled monolayer on Au(111) is shown after 2 weeks of exposure to ambient conditions. Three distinctive phases are present on the surface: the $\beta$ phase, a disordered phase, and the $\lambda$ phase (see Figure 1a). The $\beta$ phase is a centered $(23\times\sqrt{3})$ striped phase, where the decanethiolates lie flat down on the surface in an alternating head-to-head and tail-to-tail registry. The interstripe distance is approximately 3.3 nm, whereas the periodicity along the stripes is 0.49 nm ($\sqrt{3}$ times the Au(111) lattice constant (2.884 Å)). The stripes in the $\beta$ phase can shift perpendicular to the row direction by roughly half of the row spacing. The $\lambda$ phase is only observed after air-oxidation of the SAM[18] (Figure 1e shows a zoomed image of the $\lambda$ phase). This phase is ordered in a lammelae-like fashion, where the decanethiols are converted into decanesulfonates (the sulfur end-group is oxidized). The fine striped domains are approximately 3.5-nm-wide separated by vacancy lines, which run perpendicular to the fine stripes. The separation of the stripes within the lammelae is $\sqrt{3}a$ while the stripes across the vacancy line are


https://dx.doi.org/10.1021/acs.jpcc.0c02806
J. Phys. Chem. C 2020, 124, 11977−11984

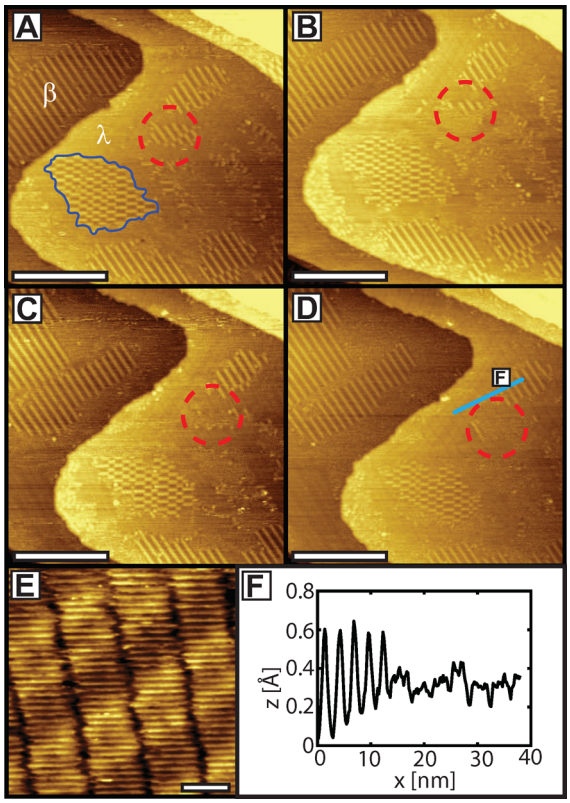


**Figure 1.** (A–D) Sequence of STM topography images (70 × 70 nm$^2$, scale bar 25 nm) of decanethiol SAM on Au(111) after 2 weeks of exposure to ambient conditions. Both the $\beta$ and a disordered phase are present on the surface. The different domains of decanethiol phases are divided by an oxidized decanethiol phase ($\lambda$ phase). The tunneling parameters are 190 pA and 1.20 V. (E) Zoomed image (20 × 20 nm$^2$, scale bar 3 nm) of the $\lambda$ phase. The herringbone reconstruction of the Au(111) surface is preserved indicating a weak interaction between the molecules and the surface. Tunneling current 55 pA, sample bias 200 mV. (F) Cross-sectional height profile from corresponding line segment in (D) shows a 33 Å corrugation periodicity of the $\beta$ phase and a 3.5 nm width of the fine stripe domains in the $\lambda$ phase.

always registered out-of-phase. The stripes run along the closed-packed direction of the Au(111) substrate ($\langle 01\bar{1}\rangle$) and make an angle of 30° with the ridges of the herringbone reconstruction (which run in $\langle 11\bar{2}\rangle$ directions). The fact that the herringbone reconstruction is still visible and unaffected by the SAM implies a weak interaction between the Au(111) surface and the molecules.[47,48] The herringbone reconstruction contains 23 atoms in the top layer placed on 22 atoms on the second layer resulting in a $(22\times\sqrt{3})$ unit cell.[49] Both *fcc* and *hcp* domains are included in an alternating order, leading to a slightly elevated ridge with a height of about 15 pm. When molecules interact with the herringbone reconstructed surface, both the *fcc*/*hcp* ratio and the unit cell become gradually larger until the reconstruction is completely lifted.[47,48] For the $\lambda$ phase, both of the effects are not observed, indicating a rather weak interaction between the molecules and the Au(111) surface.

The height variation within the $\lambda$ phase is much smaller as compared to the $\beta$ phase (see Figure 1F). In a previous study,[18] we explained this difference in terms of mixing of the sulfur orbitals. In the $\beta$ phase, the orbitals of the sulfur atoms and the gold surface mix, leading to a bright appearance in the STM images.[50] When sulfur atoms react with oxygen atoms, as is the case in the $\lambda$ phase, no mixing of orbitals occurs, and therefore smaller height differences are measured. These results are in line with measurements of the apparent barrier height, which reveal almost no contrast between the heads and the tails.

A closer look at the series of images in Figure 1A–D reveals that the decanethiol monolayers are structurally not stable. For instance, the $\beta$ island (marked with the red dashed circle) completely transforms into the disordered phase. In order to exclude tip-induced dynamics, the bias and set-point current are varied. No dependence was found between the tunneling conditions and the dynamics ($V$ is varied from 1 to 1.5 V, $I$ is varied from 50 pA to 500 pA). In Figure 2A, the relative total

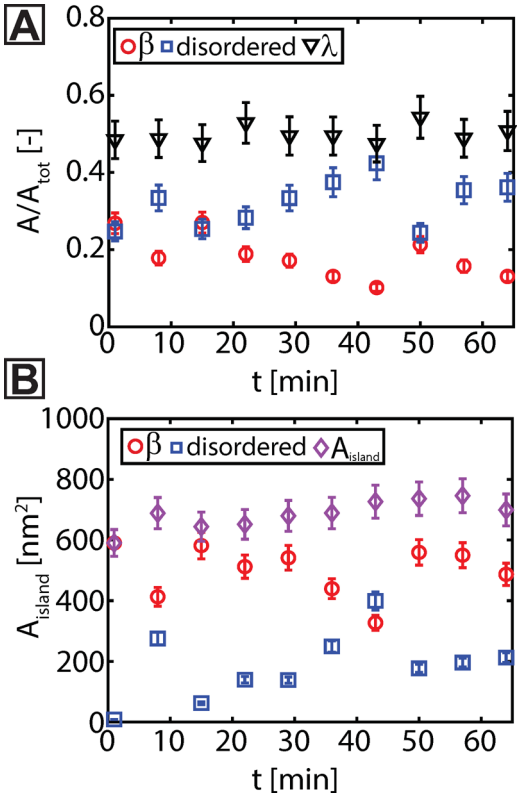


**Figure 2.** (A) Relative area of the different phases on the upper terrace as a function of time. While the area of the $\beta$ and the disordered phase vary, the $\lambda$ area remains constant. (B) Area content and total area of the island (marked in blue) in Figure 1A as a function of time. The content of the island substantially fluctuates, while the total island area remains constant, indicating that there is almost no molecular exchange with the surrounding $\lambda$ phase.

area of the $\beta$, $\lambda$, and disordered phase is plotted versus time. Surprisingly, only spatial variations are observed for the $\beta$ and the disordered phase, while the total area of the $\lambda$ phase remains roughly constant. A clear inverse correlation is observed between the $\beta$ and the disordered phase, implying that the $\beta$ phase converts to the disordered phase and vice versa. The same behavior is observed when the structural content of the island (marked with the white line in Figure 1A) is monitored as a function of time (see Figure 2B). Again, an inverse correlation is observed between the $\beta$ and the disordered phase, while the total area of the island remains practically constant. From these two observations, the following conclusions can be drawn: (1) The $\lambda$ phase is


https://dx.doi.org/10.1021/acs.jpcc.0c02806
J. Phys. Chem. C 2020, 124, 11977–11984

structurally more stable compared to the $\beta$ phase, and (2) there is limited exchange between the decanethiol ($\beta$ and disordered phase) and the air-oxidized decanethiol ($\lambda$ phase) phases.

Current−time (denoted as $I(t)$) spectroscopy is another technique to investigate structural variations on the nanoscale.[16,32,33,35,51−53] In Figure 3a, an STM image of a freshly prepared decanethiol SAM on Au(111) is shown. Both the $\beta$ and $\delta$ phases coexist on the surface in agreement with previous studies.[7,10,16,17] Figure 3b,c shows $I(t)$ traces recorded on the $\beta$ phase and the disordered phase, respectively. The set-points were fixed at 200 pA and 1.2 V. The $I(t)$ spectroscopy performed on the disordered phase (see Figure 3c) exhibits a rich dynamic behavior and extremely high current values. The current profile can be understood by the fact that molecules diffuse in and out of the tunnel junction. When the alkyl tail of the molecule flips up and makes contact with the tip, the current increases rapidly due to the different tunneling path.[35]

The $I(t)$ trace performed on the $\beta$ phase reveals a two-level switching process (see Figure 3b) independent of the probe location. The origin of the fluctuations in the current can be attributed to several dynamic processes, such as diffusion of the molecules or wagging of the alkyl tails. In the case of wagging of the alkyl tail, larger current fluctuations are expected.[35,54] Also in the case of diffusion in which a molecule moves outside the probed surface region, larger current fluctuations have been observed compared to the fluctuations measured on the $\beta$ phase (see Figure 3b).[51] Changes in the molecular configuration is another mechanism resulting in current fluctuations.[32,33,52,53] The height of the current fluctuations measured in these studies[32,33,52,53] is on the same order of magnitude as measured on the $\beta$ phase. Therefore, the molecule does not diffuse away from the tip, but simply another part of the decanethiol molecule is probed. As shown in a previous study,[16] the decanethiol SAM exhibits collective molecular diffusion, where the molecular phase is moving collectively over the surface. As a result, the sulfur head or the alkyl tail is probed resulting in two current levels. In addition, as the $\beta$ phase is moving collectively over the surface, the current fluctuations are nonlocalized, which explains why the current fluctuations are probed over the entire $\beta$ phase.

In contrast to the decanethiol phases, $I(t)$ spectroscopy on the air-oxidized decanethiols is more localized. In Figure 4a, an STM image of an air-oxidized decanethiol SAM on Au(111) is shown. Within the image, a spatially resolved activity map of 120 individual $I(t)$ traces is presented. The color map is a measure of the number of current switches per time interval, red (blue) refers to a large (small) number of current switches. When the tip is positioned at the middle of the fine stripes (blue area), only occasional current fluctuations are observed (Figure 4b shows a characteristic $I(t)$ trace on top of a fine

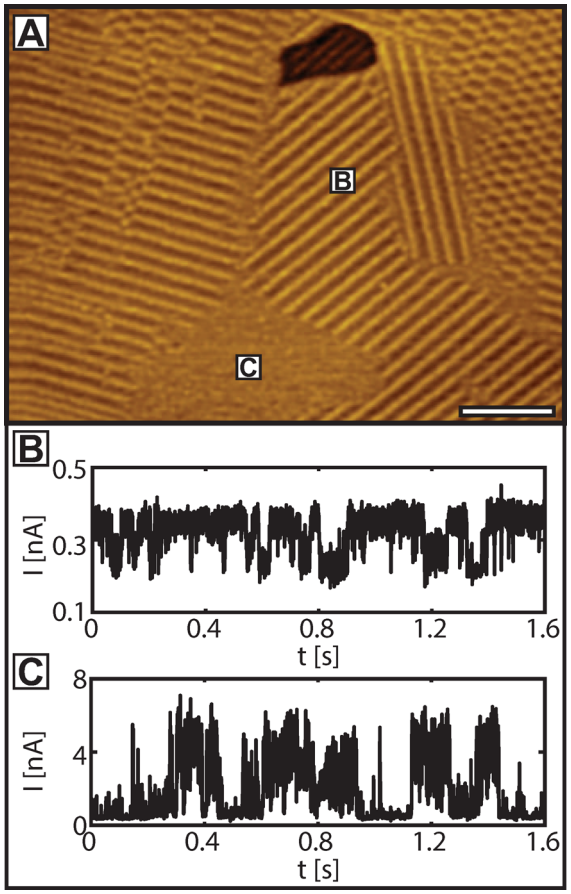


**Figure 3.** (A) STM topography image (100 × 75 nm$^2$, scale bar 15 nm) of a decanethiol SAM on Au(111) showing the various phases at room temperature. Most of the terraces are covered by the $\beta$ or the $\delta$ phase. Occasionally, a disordered phase is present on the surface. The tunneling parameters are 190 pA and 1.20 V. (B) $I(t)$ spectroscopy performed the bright stripe of the $\beta$ phase and (C) on the disordered phase.

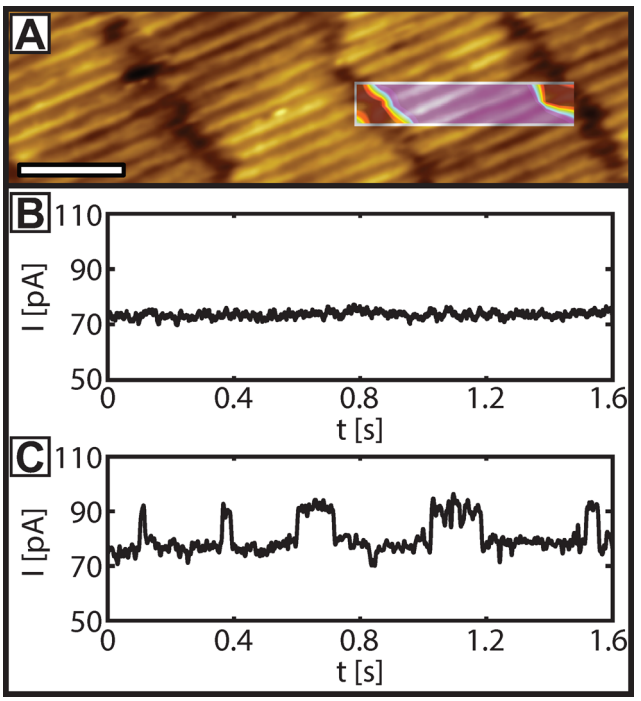


**Figure 4.** (A) STM topography image of the air-oxidized decanethiol phase (15 × 5 nm$^2$, scale bar 2 nm) with a two-dimensional activity map of the amount of activity as a function of position for 120 individual $I(t)$ traces as an overlay. The color spectrum scales from dynamic (red), many current fluctuations, to static (blue), constant current. (B) An exemplary $I(t)$ trace recorded on the molecular stripes (blue area of the activity map). (C) Characteristic $I(t)$ trace recorded on the vacancy lines between the molecule stripes (red area of the activity map). The set-points are 75 pA and 200 mV.



https://dx.doi.org/10.1021/acs.jpcc.0c02806
J. Phys. Chem. C 2020, 124, 11977−11984

stripe (blue area)). In line with the observations in Figure 2, the physisorbed decanesulfonates show no current fluctuations, indicating that the molecules are lying statically on the surface in contrast to the chemisorbed decanethiol phases. When the tip is located in the vacancy line (red area), the current flips back and forth between two well-defined levels (Figure 3c shows a characteristic $I(t)$ trace taken at a vacancy line (red area)). However, the current fluctuations are much smaller compared to the fluctuations observed in the disordered phase and one order smaller compared to the $\beta$ phase.

The fact that the herringbone reconstruction is still unaffected means that the interaction energy between the decanesulfonate is much weaker compared to the decanethiol, which makes a covalent Au−S bond with the surface. Mete et al.[37] calculated the binding/adsorption energies of a physisorbed and a chemisorbed decanethiol molecule and found −1.32 and −3.03 eV, respectively.[55] Although the decanethiol has a much stronger binding energy with the gold surface, it exhibits much greater dynamics. This is caused by the weakening of the Au−Au bonds as a consequence of the formation of the strong Au−S bond between the decanethiol and the gold adatom. Figure 5 shows the relative potential

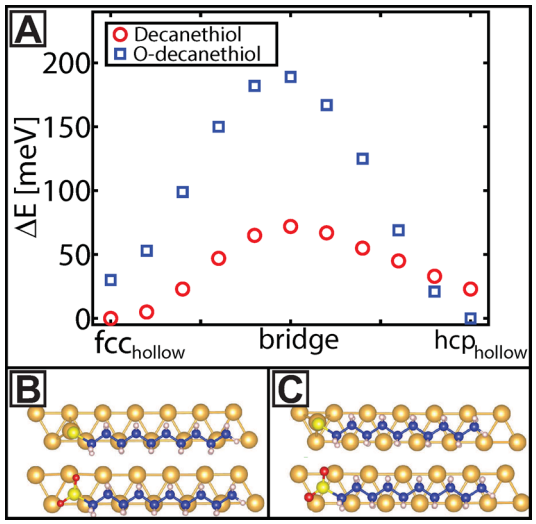


**Figure 5.** (A) Calculated potential energy for decanethiol adsorbed on the adatom (red ○) and oxidized decanethiol (blue □) as a function of the surface site. (B) Atomic model of the adsorption configuration of the decanethiol on the adatom (top) and oxidized decanethiol (bottom) on the *fcc* position. (C) Atomic model of the adsorption configuration of the decanethiol on the adatom (top) and oxidized decanethiol (bottom) on the *hcp* position. Color code: Au = gold, S = yellow, C = blue, H = white, O = red.

energies calculated on the different sites taking as a reference the most stable site. The most stable structure was found when the Au-SR complex (the gold-decanethiol complex) is positioned on the *fcc* site. Note that the S atom is always located above a Au adatom, when the atom moves from *fcc* to *hcp* site. The difference between *fcc* and *hcp* hollow sites is 23 meV. The activation barriers for diffusion from *fcc* to *hcp* and vice versa are 72 and 49 meV, respectively. These barriers are 1 order of a magnitude smaller compared to the diffusion of a bare decanethiol (without a Au adatom) on Au(111) and twice as small as the barriers for the diffusion of Au adatom on Au(111).[55] Therefore, the Au-RS complex is very mobile on the surface and explains the observed dynamic behavior of the disordered and $\beta$ phase, in agreement with previous studies.[56,57]

The situation is different for the decanesulfonates. When the sulfur atom of the decanethiol is oxidized, no covalent Au−S bond is formed and the herringbone reconstruction remains intact. The most stable structure was found when the S atom is located on top of the *hcp* site. The difference between the *hcp* and the *fcc* sites is 30 meV, comparable to the Au-SR complex. However, the activation barrier is significantly larger in the case of the decanesulfonates (the activation barrier for diffusion from *hcp* to *fcc* (*fcc* to *hcp*) is 189 (159) meV), and therefore, the decanesulfonate phase is structurally more stable, although it is only physisorbed on the surface.

The $I(t)$ spectroscopy traces on both the sulfur atoms of the $\beta$ phase and the oxidized sulfur group of the $\lambda$ phase exhibits a two-level switching process. However, the frequency of switching in the $\beta$ phase is much higher as compared to the $\lambda$ phase. For the $\beta$ and the $\lambda$ phases, a switching frequency of approximately 30 and 15 Hz is found, respectively. When the distribution of residence time ($\tau$) is plotted on a semi-logarithmic scale in Figure 6, both systems exhibit a linear

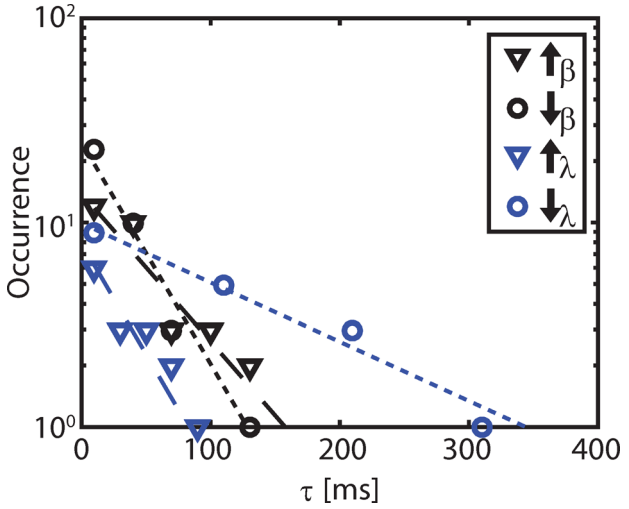


**Figure 6.** Distribution of the residence time ($\tau$) of the "up" (↑) and "down" (↓) states of the $\beta$ and $\lambda$ phase (extracted from the $I(t)$ spectroscopy) on a semilog scale. A clear preference for the "down" configuration is found for the $\lambda$ phase. The dashed lines are theoretical fits for a stochastic process (Poisson distribution).

dependence, characteristic for a stochastic, i.e., random, process.[32,33] From the slope of the curves, the average residence time ($\langle\tau\rangle$) can be extraced. For the $\beta$ phase, the residence times for the "up" and the "down" states are equal to approximately 50 ms, whereas in the case of the $\lambda$ phase, a clear preference for the "down" configuration is found (the average residence times of the "up" and "down" states are approximately 40 and 150 ms, respectively). In case of the $\beta$ phase, the collective molecular motion is the reason for the fluctuations. As the diffusion barrier is low, there is no preferred adsorption site, and therefore the "up" and the "down" configurations are about equally probable. On the other hand, in the $\lambda$ phase the molecules are static, and most probably, the current fluctuations are caused by a hindered rotation around the molecular axis of the oxidized sulfur head. As the sulfur head contains three oxygen atoms, the preferred configuration is one oxygen pointing toward the surface, while


https://dx.doi.org/10.1021/acs.jpcc.0c02806
J. Phys. Chem. C 2020, 124, 11977−11984

the tip is above the sulfur atom. When the head rotates, the oxygen atom points upward and decreases the tip−molecule distance leading to an increase in the current.

Although ease of preparation and stability of alkanethiols SAMs on gold are thus far unmatched by any other system for SAM formation, the monolayers are not ultrarobust and stable at ambient conditions. The oxidation leads to lower density decanethiol phases, which are highly dynamic due to the low activation barrier for diffusion. This is highly undesirable for ambient condition electronics or stabilization of nanoparticles. In the oxidized decanethiol SAMs almost no structural fluctuations are observed within the monolayer at room temperature, and it remains stable in ambient conditions (as the molecules are already oxidized). However, further research is needed to show that decanesulfonate self-assembled monolayers are chemically stable when the self-assembled monolayer comes in contact with other molecules.

## CONCLUSIONS

In conclusion, the dynamic behavior of decanethiol and air-oxidized decanethiol SAMs (decanesulfonates) on Au(111) has been investigated using scanning tunneling microscopy and current−time scanning tunneling spectroscopy. Surprisingly, the physisorbed decanesulfonate phase is structurally more stable compared to the chemisorbed decanethiol phase. This is due to a 100 meV difference in the diffusion barrier between the physisorbed and the chemisorbed phase. Due to the strong covalent bond between the sulfur head and the Au surface, the Au−Au bond is weakened leading to a very low activation barrier of the Au-decanethiolate complex. In the case of the decanesulfonate phase, the sulfur head is oxidized, and therefore, the sulfur head is unable to make a covalant bond with the Au surface leading to a very stable structure. A two-dimensional activity map of individual current−time traces reveals that all the dynamics take place within the vacancy lines. These results reveal that the oxidation of thiols provides a pathway to produce more robust and stable self-assembled monolayers at ambient conditions.

## AUTHOR INFORMATION


### Corresponding Author

**Kai Sotthewes** − *Physics of Interfaces and Nanomaterials, MESA+ Institute for Nanotechnology, University of Twente, 7500AE Enschede, The Netherlands;* orcid.org/0000-0003-2073-6958; Email: k.sotthewes@utwente.nl

### Authors

**Özlem Kap** − *Physics of Interfaces and Nanomaterials, MESA+ Institute for Nanotechnology, University of Twente, 7500AE Enschede, The Netherlands; Department of Materials Science and Engineering, Izmir Institute of Technology, Urla 35430, İzmir, Turkey;* orcid.org/0000-0002-7609-4272

**Nikolai Kabanov** − *Physics of Interfaces and Nanomaterials, MESA+ Institute for Nanotechnology, University of Twente, 7500AE Enschede, The Netherlands; Faculty of Physics, Lomonosov Moscow State University, Moscow 119991, Russian Federation*

**Martina Tsvetanova** − *Physics of Interfaces and Nanomaterials, MESA+ Institute for Nanotechnology, University of Twente, 7500AE Enschede, The Netherlands*

**Canan Varlikli** − *Department of Photonics, Izmir Institute of Technology, Urla 35430, İzmir, Turkey;* orcid.org/0000-0002-1081-0803

**Andrey L. Klavsyuk** − *Faculty of Physics, Lomonosov Moscow State University, Moscow 119991, Russian Federation*

**Harold J. W. Zandvliet** − *Physics of Interfaces and Nanomaterials, MESA+ Institute for Nanotechnology, University of Twente, 7500AE Enschede, The Netherlands;* orcid.org/0000-0001-6809-139X

Complete contact information is available at: https://pubs.acs.org/10.1021/acs.jpcc.0c02806


### Author Contributions

¶Ö.K. and N.K. equally contributed.

### Notes

The authors declare no competing financial interest.

## ACKNOWLEDGMENTS

The authors thank B. Poelsema for many valuable discussions and the Stichting voor Fundamenteel Onderzoek der Materie (FOM, 11PR2900) for financial support. O. K. also thanks TUBITAK (The Scientific and Technological Research Council of Turkey) for the research support with the 2214/A International Doctoral Research Fellowship. The theoretical calculations are carried out using the equipment of the shared research facilities of HPC computing resources at Lomonosov Moscow State University.

## REFERENCES


(1) Ulman, A. Formation and Structure of Self-Assembled Monolayers. *Chem. Rev.* **1996**, *96*, 1533−1554.

(2) Love, J.; Estroff, L.; Kriebel, J.; Nuzzo, R.; Whitesides, G. Self-Assembled Monolayers of Thiolates on Metals as a Form of Nanotechnology. *Chem. Rev.* **2005**, *105*, 1103−1170.

(3) Vericat, C.; Vela, M. E.; Corthey, G.; Pensa, E.; Cortes, E.; Fonticelli, M. H.; Ibanez, F.; Benitez, G. E.; Carro, P.; Salvarezza, R. C. Self-Assembled Monolayers of Thiolates on Metals: a Review Article on Sulfur-Metal Chemistry and Surface Structures. *RSC Adv.* **2014**, *4*, 27730−27754.

(4) Chaki, N. K.; Vijayamohanan, K. Self-Assembled Monolayers as a Tunable Platform for Biosensor Applications. *Biosens. Bioelectron.* **2002**, *17*, 1−12.

(5) McCreery, R. L. Molecular Electronic Junctions. *Chem. Mater.* **2004**, *16*, 4477−4496.

(6) Nerngchamnong, N.; Wu, H. R.; Sotthewes, K.; Yuan, L.; Cao, L.; Roemer, M.; Lu, J.; Ping Loh, K.; Troadec, C.; Zandvliet, H. J. W.; et al. Supramolecular Structure of Self-Assembled Monolayers of Ferrocenyl Terminated n-Alkanethiolates on Gold Surfaces. *Langmuir* **2014**, *30*, 13447−13455.

(7) Poirier, G. E. Coverage-Dependent Phases and Phase Stability of Decanethiol on Au(111). *Langmuir* **1999**, *15*, 1167−1175.

(8) Poirier, G. E.; Fitts, W. P.; White, J. M. Two-Dimensional Phase Diagram of Decanethiol on Au(111). *Langmuir* **2001**, *17*, 1176−1183.

(9) Fitts, W.; White, J.; Poirier, G. Low-Coverage Decanethiolate Structure on Au(111): Substrate Effects. *Langmuir* **2002**, *18*, 1561−1566.

(10) Qian, Y.; Yang, G.; Yu, J.; Jung, T.; Liu, G. Structures of Annealed Decanethiol Self-Assembled Monolayers on Au(111): An Ultrahigh Vacuum Scanning Tunneling Microscopy Study. *Langmuir* **2003**, *19*, 6056−6065.

(11) Burgi, T. Properties of the gold−sulphur interface: from self-assembled monolayers to clusters. *Nanoscale* **2015**, *7*, 15553.

(12) Jackson, A. M.; Myerson, J. W.; Stellacci, F. Spontaneous Assembly of Subnanometreordered Domains in the Ligand Shell of Monolayer-Protected Nanoparticles. *Nat. Mater.* **2004**, *3*, 330−336.

(13) Stranick, S.; Parikh, A.; Allara, D.; Weiss, P. A New Mechanism for Surface Diffusion: Motion of a Substrate-Adsorbate Complex. *J. Phys. Chem.* **1994**, *98*, 11136−11142.

(14) Seo, S.; Lee, H. Thermal-Processing-Induced Structural Dynamics of Thiol Self-Assembly in Solution. *J. Phys. Chem. C* **2011**, *115*, 15480−15486.
(15) Ito, E.; Kang, H.; Lee, D.; Park, J. B.; Hara, M.; Noh, J. Spontaneous Desorption and Phase Transitions of Self-Assembled Alkanethiol and Alicyclic Thiol Monolayers Chemisorbed on Au(111) in Ultrahigh Vacuum at Room Temperature. *J. Colloid Interface Sci.* **2013**, *394*, 522−529.
(16) Wu, H. R.; Sotthewes, K.; Kumar, A.; Vancso, G. J.; Schön, P. M.; Zandvliet, H. J. W. Dynamics of Decanethiol Self-Assembled Monolayers on Au(111) Studied by Time-Resolved Scanning Tunneling Microscopy. *Langmuir* **2013**, *29*, 2250−2257.
(17) Sotthewes, K.; Wu, H. R.; Kumar, A.; Vancso, G. J.; Schön, P. M.; Zandvliet, H. J. W. Molecular Dynamics and Energy Landscape of Decanethiolates in Self-Assembled Monolayers on Au(111) Studied by Scanning Tunneling Microscopy. *Langmuir* **2013**, *29*, 3662−3667.
(18) Sotthewes, K.; Kap, O.; Wu, H.; Thompson, D.; Huskens, J.; Zandvliet, H. Ordering of Air-Oxidized Decanethiols on Au(111). *J. Phys. Chem. C* **2018**, *122*, 8430−8436.
(19) Garrell, R. L.; Chadwick, J. E.; Severance, D. L.; McDonald, N. A.; Myles, D. C. Adsorption of Sulfur Containing Molecules on Gold: The Effect of Oxidation on Monolayer Formation and Stability Characterized Experiments and Theory. *J. Am. Chem. Soc.* **1995**, *117*, 11563−11571.
(20) Horn, A. B.; Russell, D. A.; Shorthouse, L. J.; Simpson, T. R. E. Ageing of Alkanethiol Self-Assembled Monolayer. *J. Chem. Soc., Faraday Trans.* **1996**, *92*, 4759−4762.
(21) Scott, J. R.; Baker, L. S.; Everett, W. R.; Wilkins, C. L.; Fritsch, I. Fritsch Laser Desorption Fourier Transform Mass Spectrometry Exchange Studies of Air-Oxidized Alkanethiol Self-Assembled Monolayers on Gold. *Anal. Chem.* **1997**, *69*, 2636−2639.
(22) Schoenfisch, M. H.; Pemberton, J. E. Air Stability of Alkanethiol Self-Assembled Monolayers on Silver and Gold Surfaces. *J. Am. Chem. Soc.* **1998**, *120*, 4502−4513.
(23) Willey, T. M.; Vance, A. L.; van Buuren, T.; Bostedt, C.; Terminello, L. J.; Fadley, C. S. Rapid Degradation of Alkanethiol-Based Self-Assembled Monolayers on Gold in Ambient Laboratory Conditions. *Surf. Sci.* **2005**, *576*, 188−196.
(24) Zhang, Y.; Terrill, R. H.; Tanzer, T. A.; Bohn, P. W. Ozonolysis Is the Primary Cause of UV Photooxidation of Alkanethiolate Monolayers at Low Irradiance. *J. Am. Chem. Soc.* **1998**, *120*, 2654−2655.
(25) Poirier, G. E.; Herne, T. M.; Miller, C. C.; Tarlov, M. J. Molecular-Scale Characterization of the Reaction of Ozone with Decanethiol Monolayers on Au(111). *J. Am. Chem. Soc.* **1999**, *121*, 9703−9711.
(26) Hutt, D. A.; Leggett, G. J. Influence of adsorbate ordering on rates of UV photooxidation of self-assembled monolayers. *J. Phys. Chem.* **1996**, *100*, 6657−6662.
(27) Lee, M.-T.; Hsueh, C.-C.; Freund, M. S.; Ferguson, G. S. Air Oxidation of Self-Assembled Monolayers on Polycrystalline Gold: The Role of the Gold Substrate. *Langmuir* **1998**, *14*, 6419−6423.
(28) Wang, M. C.; Liao, J. D.; Weng, C. C.; Klauser, R.; Shaporenko, A.; Grunze, M.; Zharnikov, M. Modification of Aliphatic Monomolecular Films by Free Radical Dominant Plasma: The Effect of the Alkyl Chain Length and the Substrate. *Langmuir* **2003**, *19*, 9774−9780.
(29) Cortes, E.; Rubert, A. A.; Benitez, G.; Carro, P.; Vela, M. E.; Salvarezza, R. C. Enhanced Stability of Thiolate Self-Assembled Monolayers (SAMs) on Nanostructured Gold Substrates. *Langmuir* **2009**, *25*, 5661−5666.
(30) Toerker, M.; Staub, R.; Fritz, T.; Schmitz-Hbsch, T.; Sellam, F.; Leo, K. Annualed Decanethiol Monolayers on Au(111): Intermediate Phases Between Structures with High and Low Molecular Surface Denisty. *Surf. Sci.* **2000**, *445*, 100−108.
(31) Schreiber, F. Structure and Growth of Self-Assembling Monolayers. *Prog. Surf. Sci.* **2000**, *65*, 151−257.
(32) Schaffert, J.; Cottin, M. C.; Sonntag, A.; Karacuban, H.; Bobisch, C. A.; Lorente, N.; Gauyacq, J. P.; Möller, R. Imaging the Dynamics of Individually Adsorbed Molecules. *Nat. Mater.* **2013**, *12*, 223−227.
(33) Sotthewes, K.; Heimbuch, R.; Zandvliet, H. J. W. Dynamics of Copper-Phthalocyanine Molecules on Au/Ge(001). *J. Chem. Phys.* **2015**, *143*, 134303.
(34) Gao, J.; Li, F.; Zhu, Z.; Yang, G.; Lu, H.; Lin, H.; Li, Q.; Li, Y.; Pan, M.; Guo, Q. Spontaneous Breaking and Remaking of the RS-Au-SR Staple in Self-Assembled Ethulthiolate/Au(111) Interface. *J. Phys. Chem. C* **2018**, *122*, 19473.
(35) Sotthewes, K.; Geskin, V.; Heimbuch, R.; Kumar, A.; Zandvliet, H. J. W. Research Update: Molecular Electronics: The Single-Molecule Switch and Transistor. *APL Mater.* **2014**, *2*, 010701.
(36) Lavrich, D. J.; Wetterer, S. M.; Bernasek, S. L.; Scoles, G. Physisorption and Chemisorption of Alkanethiols and Alkyl Sulfides on Au(111). *J. Phys. Chem. B* **1998**, *102*, 3456−3465.
(37) Mete, E.; Yortanli, M.; Danisman, M. F. A van der Waals DFT Study on Chain Length Dependence of Alkanethiol Adsorption on Au(111): Physisorption vs. Chemisorption. *Phys. Chem. Chem. Phys.* **2017**, *19*, 13756−13766.
(38) Blöchl, P. E. Projector Augmented-Wave Method. *Phys. Rev. B: Condens. Matter Mater. Phys.* **1994**, *50*, 17953−17979.
(39) Kresse, G.; Joubert, D. From Ultrasoft Pseudopotentials to the Projector Augmented-Wave Method. *Phys. Rev. B: Condens. Matter Mater. Phys.* **1999**, *59*, 1758.
(40) Kresse, G.; Hafner, J. Ab Initio Molecular Dynamics for Liquid Metals. *Phys. Rev. B: Condens. Matter Mater. Phys.* **1993**, *47*, 558−561.
(41) Perdew, J. P.; Burke, K.; Ernzerhof, M. Generalized Gradient Approximation Made Simple. *Phys. Rev. Lett.* **1996**, *77*, 3865−3868.
(42) Monkhorst, H. J.; Pack, J. D. Special Points for Brillouin-Zone Integrations. *Phys. Rev. B* **1976**, *13*, 5188.
(43) Steinmann, S. N.; Corminboeuf, C. Comprehensive Benchmarking of a Density-Dependent Dispersion Correction. *J. Chem. Theory Comput.* **2011**, *7*, 3567−3577.
(44) Henkelman, G.; Jonsson, H. Improved Tangent Estimate in the Nudged Elastic Band Method for Finding Minimum Energy Paths and Saddle Points. *J. Chem. Phys.* **2000**, *113*, 9978.
(45) Henkelman, G.; Uberuaga, B. P.; Jonsson, H. A climbing image nudged elastic band method for finding saddle points and minimum energy paths. *J. Chem. Phys.* **2000**, *113*, 9901.
(46) Momma, K.; Izumi, F. VESTA 3 for Three-Dimensional Visualization of Crystal, Volumetric and Morphology Data. *J. Appl. Crystallogr.* **2011**, *44*, 1272−1276.
(47) Rossel, F.; Brodard, P.; Patthey, F.; Richardson, N. V.; Schneider, W.-D. Modified Herringbone Reconstruction on Au(111) Induced by Self-Assembled Azure A Island. *Surf. Sci.* **2008**, *602*, L115−L117.
(48) Jewell, A. D.; Kyran, S. J.; Rabinovich, D.; Sykes, E. C. H. Effect of Head-Group Chemistry on Surface-Mediated Molecular Self-Assembly. *Chem. - Eur. J.* **2012**, *18*, 7169−7178.
(49) Wöll, C.; Chiang, S.; Wilson, R. J.; Lippel, P. H. Determination of Atom Positions at Stacking-Fault Dislocations on Au(111) by Scanning Tunneling Microscopy. *Phys. Rev. B: Condens. Matter Mater. Phys.* **1989**, *39*, 7988−7991.
(50) Zeng, C.; Li, B.; Wang, B.; Wang, H.; Wang, K.; Jang, Y.; Jou, J.; Zhu, Q. What Can a Scanning Tunneling Microscope Image Do for the Insulating Alkanethiol Molecules on Au(111) Substrates? *J. Chem. Phys.* **2002**, *117*, 851.
(51) Stipe, B. C.; Rezaei, M. A.; Ho, W.; Gao, S.; Persson, M.; Lundqvist, B. I. Single-molecule dissociation by tunneling electrons. *Phys. Rev. Lett.* **1997**, *78*, 4410.
(52) Liu, Q.; Zhang, Y. Y.; Jiang, N.; Zhang, H. G.; Gao, L.; Du, S. X.; Gao, H. J. Identifying Multiple Configurations of Complex Molecules in Dynamical Processes: Time Resolved Tunneling Spectroscopy and Density Functional Theory Calculation. *Phys. Rev. Lett.* **2010**, *104*, 166101.
(53) Sotthewes, K.; Heimbuch, R.; Zandvliet, H. J. W. Manipulating Transport Through a Single-Molecule Junction. *J. Chem. Phys.* **2013**, *139*, 214709.


https://dx.doi.org/10.1021/acs.jpcc.0c02806
J. Phys. Chem. C 2020, 124, 11977−11984

(54) Kockmann, D.; Poelsema, B.; Zandvliet, H. J. W. Transport Through a Single Octanethiol Molecule. *Nano Lett.* **2009**, *9*, 1147−1151.
(55) Cometto, F. P.; Paredes-Olivera, P.; Macagno, V. A.; Patrito, E. M. Density Functional Theory Study of the Adsorption of Alkanethiols on Cu(111), Ag(111) and Au(111) in the Low and High Coverage Regimes. *J. Phys. Chem. B* **2005**, *109*, 21737−21748.
(56) Maksymovych, P.; Sorescu, D. C.; Yates, J. T. Gold-Adatom-Mediated Bonding in Self-Assembled Short-Chain Alkanethiolate Species on the Au(111) Surface. *Phys. Rev. Lett.* **2006**, *97*, 146103.
(57) Gao, J. Z.; Li, F. S.; Guo, Q. M. Balance of Forces in Self-Assembled Monolayers. *J. Phys. Chem. C* **2013**, *117*, 24985−24990.


https://dx.doi.org/10.1021/acs.jpcc.0c02806
*J. Phys. Chem. C* 2020, 124, 11977−11984